BNL-97191-2012-CP

Drift time variations in CdZnTe detectors measured with alpha-particles: Their correlation with the detector's responses

J. Butcher, M. Hamade, M. Petryk, A.E. Bolotnikov, G.S. Camarda, Y. Cui, A. Hossain, K. Kim, G. Yang, and R.B. James

Presented at the SORMA WEST 2012 Conference
Oakland, California
May 14 – 17, 2012

April 2012

Nonproliferation and National Security Department

Brookhaven National Laboratory
P.O. Box 5000
Upton, NY 11973-5000
www.bnl.gov

Notice: This manuscript has been authored by employees of Brookhaven Science Associates, LLC under Contract No. DE-AC02-98CH10886 with the U.S. Department of Energy. The publisher by accepting the manuscript for publication acknowledges that the United States Government retains a non-exclusive, paid-up, irrevocable, world-wide license to publish or reproduce the published form of this manuscript, or allow others to do so, for United States Government purposes.

This preprint is intended for publication in a journal or proceedings. Since changes may be made before publication, it may not be cited or reproduced without the author's permission.

DISCLAIMER

This report was prepared as an account of work sponsored by an agency of the United States Government. Neither the United States Government nor any agency thereof, nor any of their employees, nor any of their contractors, subcontractors, or their employees, makes any warranty, express or implied, or assumes any legal liability or responsibility for the accuracy, completeness, or any third party's use or the results of such use of any information, apparatus, product, or process disclosed, or represents that its use would not infringe privately owned rights. Reference herein to any specific commercial product, process, or service by trade name, trademark, manufacturer, or otherwise, does not necessarily constitute or imply its endorsement, recommendation, or favoring by the United States Government or any agency thereof or its contractors or subcontractors. The views and opinions of authors expressed herein do not necessarily state or reflect those of the United States Government or any agency thereof.

Printed on recycled paper

Drift-time variations in CdZnTe detectors measured with alpha particles: Their correlation with detector response

J. Butcher, M. Hamade, M. Petryk, A. E. Bolotnikov, G. S. Camarda, Y. Cui, A. Hossain, K. H. Kim, G. Yang and R. B. James

Brookhaven National Laboratory, Upton, NY, USA

Abstract

Homogeneity of properties related to material crystallinity is a critical parameter for achieving high-performance CdZnTe (CZT) radiation detectors. Unfortunately, this requirement is not always satisfied in today's commercial CZT material due to high concentrations of extended defects, in particular subgrain boundaries, which are believed to be part of the causes hampering the energy resolution and efficiency of CZT detectors. In the past, the effects of subgrain boundaries have been studied in Si, Ge and other semiconductors. It was demonstrated that subgrain boundaries tend to accumulate secondary phases and impurities causing inhomogeneous distributions of trapping centers. It was also demonstrated that subgrain boundaries result in local perturbations of the electric field, which affect the carrier transport and other properties of semiconductor devices. The subgrain boundaries in CZT material likely behave in a similar way, which makes them responsible for variations in the electron drift time and carrier trapping in CZT detectors. In this work, we employed the transient current technique to measure variations in the electron drift time and related the variations to the device performances and subgrain boundaries, whose presence in the crystals were confirmed with white beam X-ray diffraction topography and infrared transmission microscopy.

Keywords: CdZnTe detectors, virtual Frisch-grid detectors, crystal defects, subgrain boundaries

1. Introduction

CdZnTe (CZT) is today's most promising semiconductor material for room-temperature gamma-ray detectors. It is used in many applications, including nonproliferation, national security, medical imaging, and astrophysics [1]. However, the widespread use of CZT detectors is hampered by poor crystallinity of material that alters the device characteristics anticipated by users. Our group in Brookhaven National Laboratory (BNL) conducts systematic studies detailing the roles of crystal defects in CZT detectors and their underlying mechanisms. We routinely employ material and device characterization techniques such as infrared transmission microscopy, white beam X-ray diffraction topography, and high-spatial-resolution X-ray response mapping to identify particular types of defects and define their relationship with device performance [2-4]. Our results from screening a large number of CZT samples indicate that amongst the different types of extended defects, subgrain boundaries—which are very common in commercial CZT regardless of growth methods and manufacture—could be as critical as large-size Te inclusions, which had been previously identified as a major cause of charge-transport non-uniformity [5].

This work continues our studies of subgrain boundaries and their effects on carrier transport in CZT detectors. Following Rudolph's works [6,7] there are several types of subgrain boundaries in CZT and other compound semiconductors. In general, they are treated as arrays of dislocations aligned along planes or three-dimensional surfaces of different sizes and geometries. They can be classified based on the density of dislocations, which can range from low dislocation density walls to high dislocation density boundaries consisting of nearly polycrystalline material.

In the past, the effects of subgrain boundaries have been extensively studied in Si and Ge—two semiconductors which have drawn much attention because of their use in electronic devices. It was demonstrated that subgrain boundaries tend to accumulate secondary phases and impurities resulting in inhomogeneous distribution of trapping centers over device volumes. In addition, subgrain boundaries may cause local perturbations of the electric field, which affect carrier transport in semiconductors.

The results of our previous studies indicate that subgrain boundaries play similar roles in CZT material. Using the X-ray response mapping technique, we have shown that subgrain boundaries correlate with the areas from which the charge collection efficiency is reduced, and that the magnitude of such reductions depends on the density of dislocations located within subgrain boundaries (different contrasts are produced by subgrain boundaries with different densities of dislocations, which can be clearly seen in diffraction topographs). Furthermore, by tracing electron-cloud drift trajectories, we have demonstrated variations in local electric fields, which were correlated with subgrain boundaries as well.

One of the consequences of the electric field inhomogeneity in CZT detectors is potentially strong variations of the electron-cloud drift times. If subgrain boundaries change the magnitude and the direction of the local electric field, which is otherwise expected to be uniform in a CZT slab, the distance of total drift of the electron cloud and its average drift velocity should differ from event to event. The drift distance can be even shorter than the crystal's length if the subgrain boundary steers the electron cloud towards the crystal's side surface.

In this work, we employed transient current signals, induced by alpha particles, to evaluate variations in electron drift-time and correlate them with subgrain boundaries and the device response as measured with gamma-rays. Knowledge of a typical scale of the drift-time variations in CZT detectors is crucial because different drift times corresponding to the same drift distance can cause additional fluctuations in continuous charge loss due to trapping by point defects. Since the continuous charge loss is a function of the electron drift time only, the latter should be measured for each interaction event (instead of depths of interactions) to assure a proper charge-loss correction. The drift-time variations should also play critical roles in pixel detectors employing Compton kinematics and other algorithms for reconstructing directions of incident gamma-ray imaging and rejecting incomplete charge collection events. Kim et al. has recently reported the uncertainties in determining distances for the multiple interaction point-events resulting in poor angular resolution of 3D position sensitive pixel detectors [10].

2. Experimental setup

We used alpha particles from an ^{241}Am source to generate transient events in long, >10 mm, parallelepiped-shaped CZT crystals with cross sections of 6x6 mm^2 configured as planar detectors with monolithic contacts. Detector-grade CZT crystals with high-resistivity, >3x10^{10} Ohm-cm, high mu-tau product (>10^{-2} cm^2/V) and low concentrations of small-size Te inclusions were acquired from two vendors, Endicott Interconnects and Redlen Technologies. The vendor can control and verify these parameters; however, they cannot control and measure the content of the subgrain boundaries in their crystals.

During the measurements, a detector was mounted inside a standard eV-Product's device holder with the alpha-particle source also placed inside the holder at ~3-mm distance from the cathode. To reduce the count rate and avoid signal pileups during the measurements, we partially screened the cathode using several layers of thin metal mesh. The anode signals were read out with the charge-sensitive preamplifier eV-5093 and recorded with a LeCroy WaveRunner. The output signals from the preamplifier were also sent to the delay line amplifier used to generate triggers for the WaveRunner. Fig. 1 (a) shows a typical waveform, containing 1000 sampling points taken with 5-ns intervals.

The following algorithm was employed to evaluate the waveforms' rise times that represent the drift times of the electron clouds generated near the cathode [8]. The event's arrival time is identified approximately when the signal rises above one sigma of the baseline's noise. Due to the noise, several signal crossings may occur. To eliminate such false starting times, only the last crossing is used. The exact arrival time is calculated as an intersection of two lines: one is a forward interpolation of the baseline and the other a backward interpolation of the pulse's leading edge. Previously, we demonstrated that this method provides ~10 ns statistical uncertainty for finding the time of the interaction's occurrence. The electron cloud's arrival time to the anode is signified as the transition of the fast-rising to slow-changing slope of the pulse. However, due to several factors, this moment can not be well defined. So, we assign the arrival time as an intersection of two lines: One is the forward interpolation of the leading edge of the pulse as its amplitude raises between 65% and 90% of its maximum; and second is the backward interpolation of the slow-changing portion of the pulse (typically the last 200-400 data points).

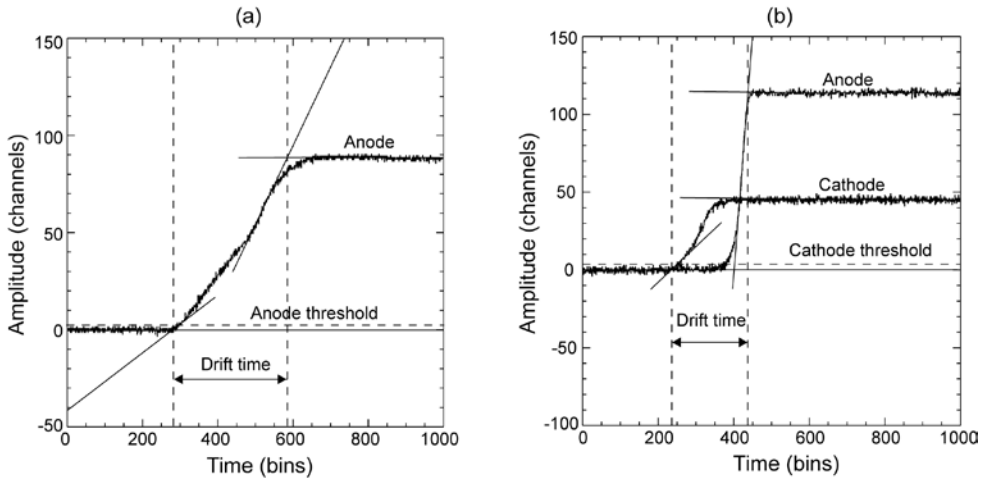

Fig. 1. Typical waveforms generated by alpha particles in a 15-mm-thick planar detector (a), and 662-keV gamma rays in a 15-mm-thik virtual Frisch-grid detector (b).

After taking the data with alpha particles, we reconfigured the CZT samples as virtual Frisch-grid detectors and acquired pulse-height spectra from the uncollimated ^{137}Cs source. A device fabrication procedure was described elsewhere [9]; we encapsulated the crystals in ultra-thin polyester shrink shells, and then placed 5-mm wide shielding electrodes around the sides near the anodes. During the measurements, a detector was placed inside a custom-made holder with two BNC connectors to apply a high-voltage bias on the cathode and to read the signals from both the cathode and anode. The signals from the cathode and the anode were recorded with the WaveRunner and digitally processed to evaluate the dependencies of the signals' amplitudes versus the electrons' drift-times (for the charge-loss correction). The measured spectra, representing the quality of the detector's responses, were correlated with the drift-time distributions, measured with alpha particles, and the X-ray diffraction topographs revealing the subgrain boundaries. To illustrate the waveform processing algorithm, Fig. 1(b) shows an example of the anode and cathode signals generated by an interaction event. We applied a similar algorithm that we used to evaluate drift times in the case of alpha-particle measurements. The cathode signals were used to calculate the interaction moments or starting moments of the electron clouds' drift. The electron clouds' arrival times to the anode were calculated by using the anode signals that have faster rising times in the virtual Frisch-grid device. The amplitudes of the cathode and anode signals were assessed by taking the differences between the baselines and the step heights averaged over 50 points. The baselines were determined by averaging the data points right before the interaction moment, while the step heights were measured with a 25-point delay after the arrival times.

We also took measurements of the electron cloud drift time variations in a 3D position sensitive 20x20x10 mm^3 detector readout with a data acquisition system based on the H3D ASIC. To plot the drift time distributions we selected the total-energy-absorption single-point-interaction events generated by 662-keV photons from the ^{137}Cs source. The descriptions of the H3D ASIC readout system and time reconstruction algorithm are given in Ref. [11].

Finally, we employed the White Beam X-Ray Diffraction Topography (WBXDT) at BNL's National Synchrotron Light Source [12] and the automated IR transmission microscopy system [13] to reveal extended defects inside the CZT detectors used in these measurements.

3. Results and Discussion

It is well known that shapes of the transient signals in CZT detectors differ from the ones that would be expected for a homogeneous detector with a uniform distribution of the electric field. In the case of the planar geometry, the rising edges in the signals reflect changes of the electron clouds drift velocity in a z-direction, which in turn corresponds to the local variations in the electric field. As we expected, our measurements demonstrated large variations in the shapes of the transient signals and electron-drift times whose magnitudes were correlated with the presence of subgrain boundaries in the CZT material. Fig. 1(a)

shows an example of a transient signal whose rising slope indicates a lowering of the electric field in the middle of the detector. We noticed that on average detectors fabricated from the Bridgman-grown material exhibit sub-linear slopes, as we would expect if the electric field gradually decays towards the anode. In contrast, the pulses in detectors fabricated from the material grown by the traveling heater method have *S*-shaped slopes suggesting that the electric field decays slightly halfway between the cathode and the anode and then regains its strength. These observations are relevant to the long-drift detectors. We note that in detectors with a planar geometry, the lateral (parallel to the anode plane) movements of the electron clouds are also seen by the anode as a slowing drift in the anode's direction.

1.1 Results from testing bar-shaped detector

The results from the measurements taken with alpha particles are summarized in Fig. 2 for three representative detectors. Shown on the left are the diffraction topographs, and on the right are the distributions of the drift times measured for two crystal orientations with respect to the cathode and anode sides. The samples' dimensions and applied biases are indicated in the plots along with the expected drift times evaluated—assuming a uniform distribution of the electric field inside the detectors—and an electron mobility of 1000 cm^2/V-s. The expected drift times are denoted as dashed lines in the drift-time distributions (plots on the right).

Analysis of the waveform data showed the experimental drift times to vary significantly from sample to sample. Judging from the diffraction topography data, the sample on top has a dense network of low dislocation-density subgrain boundaries relative to the middle and bottom samples. Accordingly, this sample shows a relatively narrow, symmetrical distribution of drift times. The tails on the right side extend up to 2000 ns indicating a slow drift for some fraction of events. The left-side tails represent the events when the electron clouds were steered to the crystal's side surfaces (edge effect), and hence, for such events the electron-drift times were shorter than expected. This feature is especially apparent in the middle and bottom samples, which revealed a distribution in the electron drift times over two peaks, as opposed to a predicted single, narrow peak. The diffraction topographs taken for these two samples demonstrated that, in addition to the network of low-dislocation-density boundaries, there were several very pronounced subgrain boundaries with high dislocation densities, which significantly distorted the crystal lattice locally. In turn, this affects the local electric field, entailing broad and multiple-peak distributions of the drift times. The presence of the high-dislocation-density boundaries can also explain the marked difference in the distributions of drift time measured for two orientations of these samples. In principle, by using the collimated source and more complex pulse-shape analysis, it is possible to trace the electron clouds' drift paths and evaluate their drift times in relation to the specific types of the subgrain boundaries and their orientations. Such measurements currently are underway.

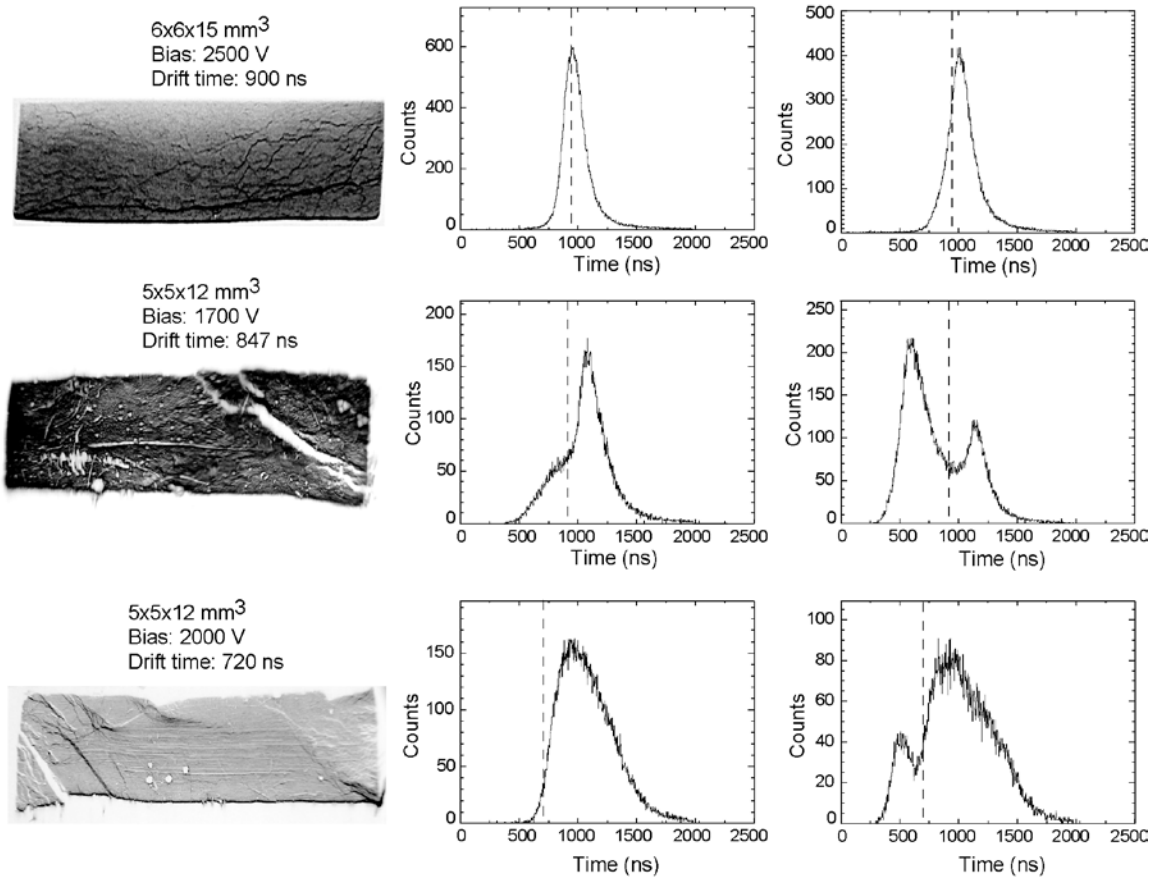

Fig. 2. Diffraction topographs (left), and the distributions of the drift times (right) measured for three representative crystals at two different orientations with respect to the cathode and anode sides. The samples' dimensions and applied biases are provided in the pictures, along with the expected drift times evaluated, assuming a uniform distribution of the electric field inside the detectors and an electron mobility of 1000 cm^2/V-s.

Many effects of the subgrain boundaries on carrier transport in semiconductor materials have been attributed to the presence of potential barriers along the boundaries, thereby changing the local electric field [14]. This likely happens in low resistivity semiconductors and devices operating at low biases. However, for high-resistivity CZT detectors with internal electric fields of > 1000 V/cm, the variations of the electric field are probably due to the formation of domains with different concentrations of accumulated space charge. The subgrain boundaries that accumulate impurities and secondary phases represent highly conductive regions in comparison to the bulk surfaces that divide the crystal volume into numerous domains. In terms of the electrostatic problem for the distribution of the electric field inside the weakly conducting bulk, we can consider the strong conducting subgrain boundaries as bounding conditions that define the electric fields inside individual domains. Accordingly, the electron clouds move across these regions with different velocities. The side surfaces of the crystals play similar roles setting the boundary conditions that shape the distribution of the electric field inside.

Our measurements indicate that, in addition to the variations of the drift times caused by random distribution of interaction points inside detectors, there are significant variations caused by differences in the electric field. If left uncorrected, both effects engender variability in charge loss due to the continuous trapping by uniformly distributed point-defects that degrade the energy resolution of the CZT detectors. Fortunately, these effects can be minimized. Since the charge loss due to continuous trapping is proportional to the drift time, we can use the latter to correct the amount of charge loss for each interaction event. We note that variations caused by the random distribution of interaction points can be corrected by

using depth-sensing techniques, e.g., by measuring the ratio of the cathode- and anode-signals as proposed for pixel detectors [15]. To rectify both effects, direct measurements of the electron-cloud drift times are required; the depth-sensing technique alone is inadequate for detectors containing networks of subgrain boundaries.

Unfortunately, variable drift times are not the only problem related to the presence of subgrain boundaries; they also cause an inhomogeneous distribution of trapping centers, which are typically assumed to be uniformly distributed inside a detector. If such non-uniformities in the CZT material are relatively small and modulated only gradually, the corresponding variations of charge loss due to trapping can be corrected partially with pixel anodes and a 3D readout scheme. However, to establish such corrections, the responses generated by the electron clouds produced in every voxel of a detector must be calibrated accurately. In general, for a certain fraction of the events, the charge loss associated with subgrain boundaries (or big Te inclusions) cannot be corrected because of the lack of a one-to-one relationship between the amount of charge loss and the drift times and voxel coordinates. Such incomplete charge-collection events may cause broadening of the photopeaks, and can primarily contribute to the continuums in the pulse-height spectra. In devices that provide information on drift time, such events can be identified and rejected from the energy spectra [16].

The effects described above are evident in the pulse-height spectra measured from the five representative virtual Frisch-grid detectors of 15- and 20-mm thicknesses (Fig. 3). These detectors were cut from the same wafer with similar distributions of Te inclusions, viz., mostly small, <5 μm. The left column in Fig. 3 contains their diffraction-topography images, the second the drift-time distribution measured with alpha particles, while the two right-most columns show the pulse-height spectra before and after correcting the drift time. As expected, the widths of the photopeak in the uncorrected spectra measured for all detectors correlate with the drift-time distributions: The wider photopeaks correspond to the wider drift-time distributions. In contrast, the photopeaks in the corrected spectra seem to correlate with the diffraction topography images. As a general trend, the dense networks of low-dislocation-density subgrain boundaries broaden the photopeaks (detectors illustrated in the second and fourth rows), while the high-dislocation-density subgrain boundaries with a few branches have little effect on the photopeaks' widths, but significantly reduce their heights or photoefficiency (detectors illustrated in the first, third, and last rows). In the latter case, the correction for charge loss improves the photopeak widths. However, we mention that it is not always possible to predict the degree of degradation of the energy resolution based on the subgrain boundaries as seen in the diffraction topographs. Similarly, as was shown in Fig. 2, for some events, the drift times are shorter than the theoretical limits indicating that the electron clouds reach the detectors' side surfaces where they become trapped. We note that the electronic noise, evaluated by applying the test pulses during the measurements (not shown in the pulse-height spectra) was < 0.8% at 662 keV for all detectors, a small value compared to the measured widths of the photopeaks.

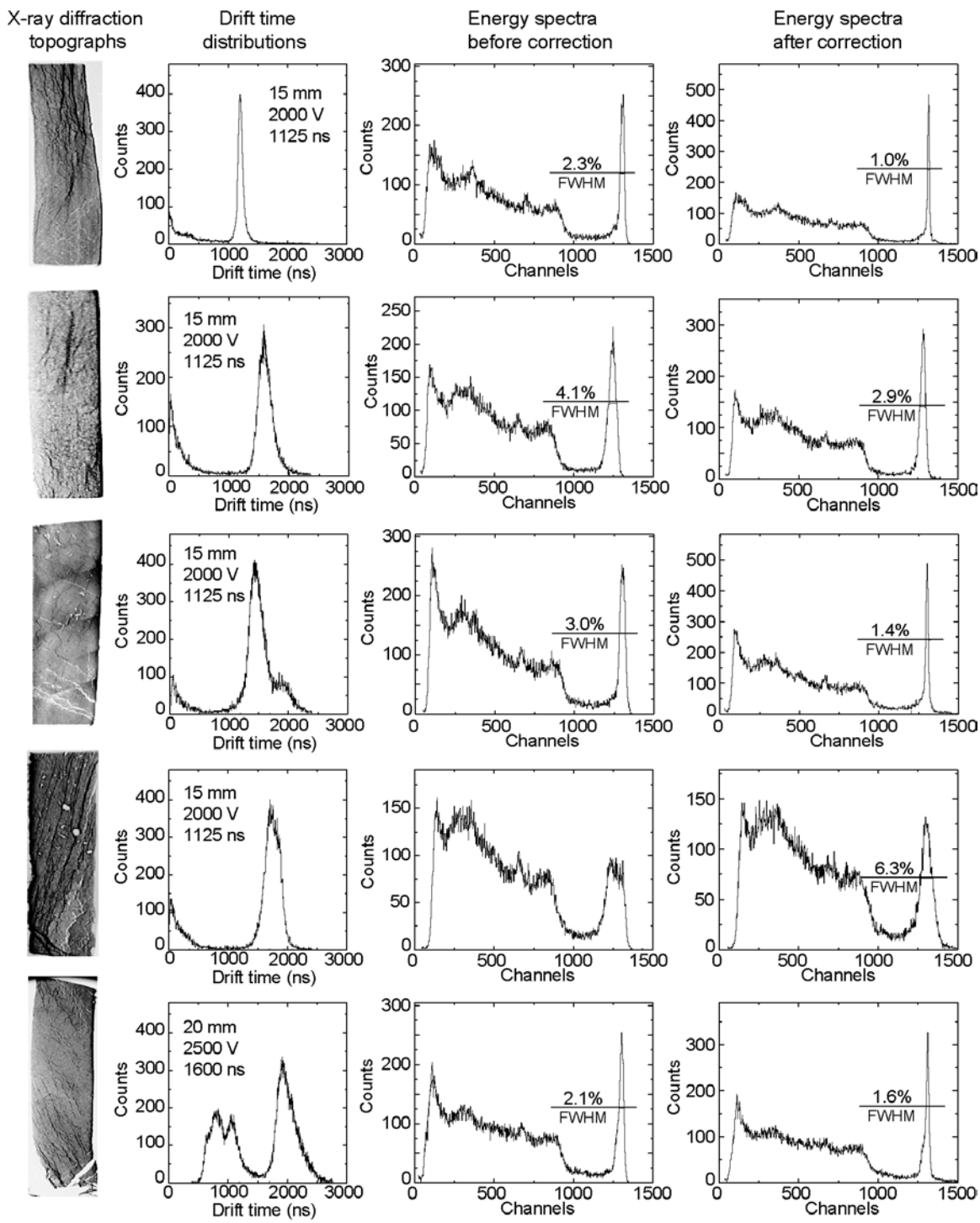

Fig. 3. Diffraction topographs, drift-time distributions, and corresponding pulse-height spectra (from right to left) measured for the five virtual Frisch-grid detectors (from top to bottom). The rightmost pulse-height spectra were corrected for charge loss due to trapping by directly measuring the drift times of the electron cloud.

1.2 Results from testing a pixel detector

The variations in drift time can cause uncertainties in determining the distances for the multiple interaction point events in pixel detectors. From this point of view, a 3D-position-sensitive detector is very convenient for measuring the local variations of the drift time in CZT crystals with poor homogeneity. Here, we tested a 10-mm thick detector biased at 800 V. The cathode- and anode-peaking times were 2 μs. We note that despite the long peaking time used in these measurements, the amplitudes of the long-rising cathode signals still suffered from the ballistic deficit. Out of 121, we selected 10 representative pixels from which we plotted dependencies of the amplitudes of the signals from the anode, *A*, and the cathode, *C*, versus drift times, *T*. Fig. 4 shows the plotted distributions *A vs. T* (right) and *C vs. T* (left) for each of the selected pixels. The plots *A vs. T* contain both the photoabsorption (photopeak) and the Compton-scattering events. We used these plots to select the photopeak events; they are represented by a narrow track of dots following the topmost edge of the continua. This was done by fitting the center of gravity of the track with a spline function, and selecting the events whose amplitudes lie within +/-1% of the fitting spline (for illustration, the fitting splines are shown for two pixels only). By selecting the photopeak events, we cut all but those events for which the numbers of generated carriers corresponded to the same deposited energy of 662 keV; the corresponding electron clouds were fully collected at the pixel anodes. In other words, the events in the *C vs. T* plots correspond to the narrow "slice" of the photopeak events in *A vs. T*. Since in a detector with planar geometry, the cathode signal is a direct measure of an interaction point's distance from the cathode, then the *C vs. T* represents the correction between the drift time and the interaction depth. In an ideal detector, such a distribution should follow a narrow line, whose width is determined by the electronic noise, while the drift time spans between 0 and its maximum value $L/\mu E$, where L, μ, and E are, respectively, the device's thickness, electron mobility, and the strength of the electric field (1250 ns in this case). In reality, as evident from Fig. 4, the measured correlations of *C vs. T* are represented by broad distributions of dots with curvatures indicating the variations of the electric field along the depth, and also within the pixel areas. For this particular detector, the midsection (between the anode and cathode) has a weaker electric field resulting in the *S*-shape of *C vs. T*. In our case, Pixel 1 exhibits almost normal behavior with a total drift time, ~1250 ns, corresponding to the 800-V bias applied to the detector, while Pixels 7-10 indicate drift times of ~1.5 times longer, with significant variations over the pixel areas.

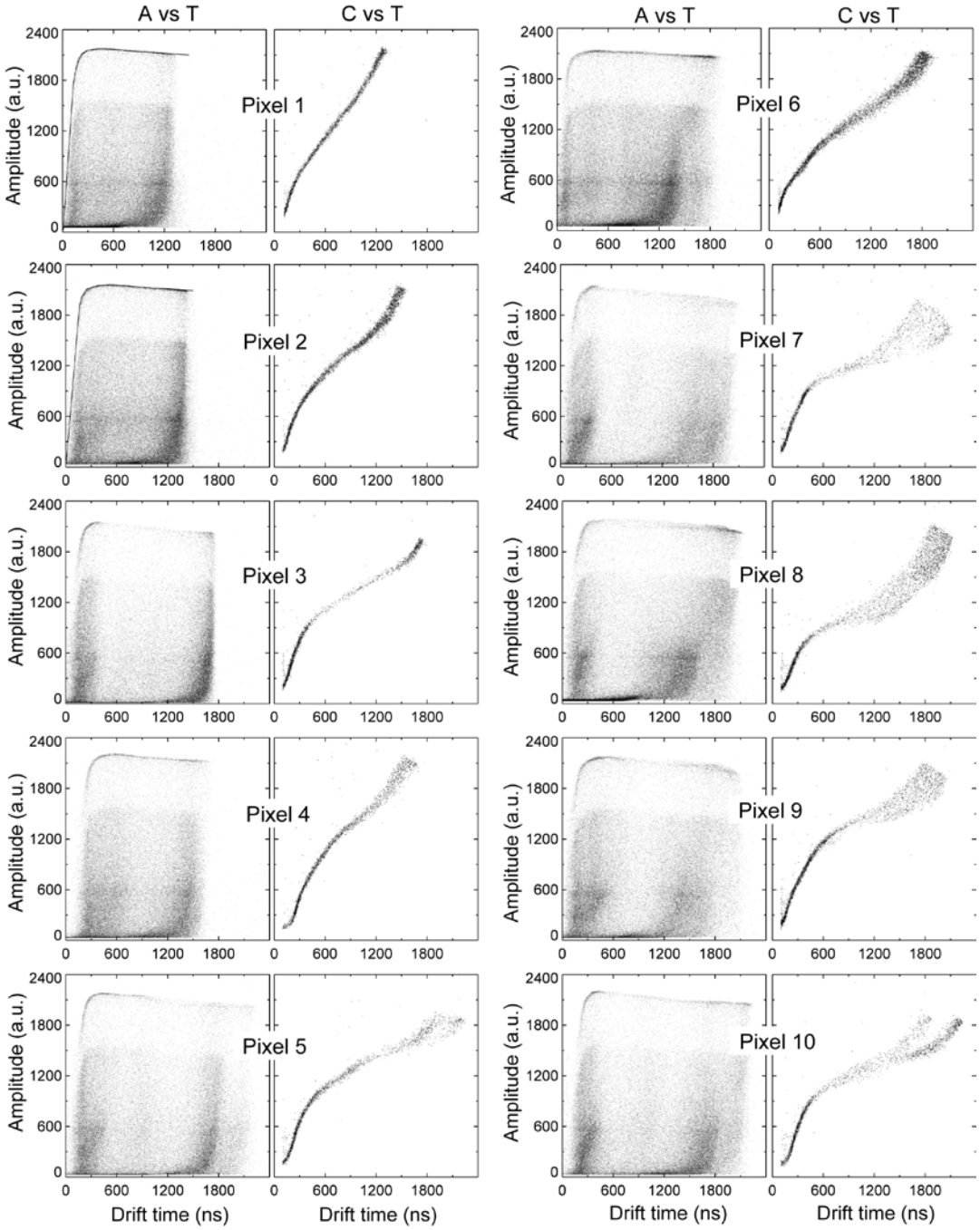

Fig. 4. Correlations of *A vs. T* (right) and *C vs. T* (left) plotted for 10 selected pixels. The distributions, *A vs. T*, contain all events (the photoabsorption (photopeak) and Compton scattering), while the distributions *C vs. T* contain only photopeak events. See text for details. The total drift time expected from this 10-mm thick detector biased at 800 V is 1250 ns.

Fig. 5 shows the inverted distributions *T vs. C* plotted for the first 9 pixels in Fig. 4. (Again, we note that the cathode signal is a measure of a Z coordinate (depth) of the interaction point.) Such distributions should be used to make corrections for variations in drift time to correctly evaluate Z-coordinates. However, if the drift time differs within the pixel areas (Pixels 4-9), such corrections may not be accurate; using a smaller pixel size can help to minimize this problem.

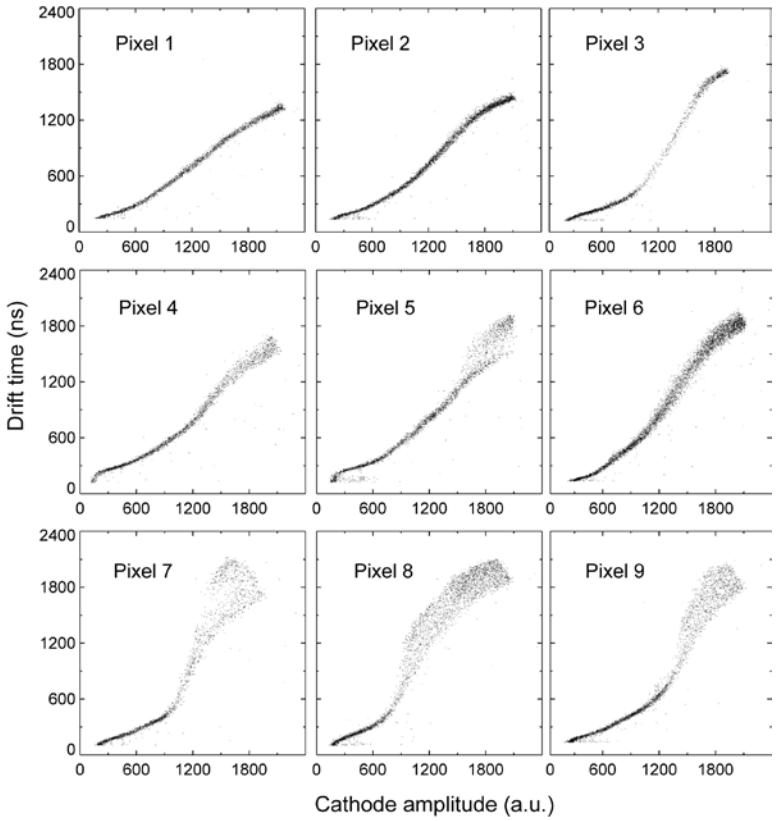

Fig. 5. Distributions of *T vs. C* plotted for the first 9 pixels shown in Fig. 4. Such distributions should be used to make corrections for the variations in drift-time variations to evaluate Z coordinates correctly.

4. Conclusions

Subgrain boundaries are critical for the performance of CZT detectors; they accumulate impurities and secondary phases that affect the detectors' energy and spatial resolution. In this work, we evaluated over 20 15- and 20-mm-thick virtual Frisch-grid detectors fabricated from CZT crystals containing subgrain boundaries, but practically free from big Te inclusions and other defects; this allowed us to neglect the effect of Te inclusions, and investigate the roles of the subgrain boundaries. We also have tested a 20x20x10 mm^3 pixel detector, which is convenient for measuring the local variations of the drift time in CZT crystals with poor homogeneity.

We employed the transient-current technique to directly measure the variations in the electron drift times and correlate them with the presence of subgrain boundaries. We used diffraction-topography images to confirm the presence of the subgrain boundaries in our samples, and linked them to the distribution of drift times and the detectors' responses to gamma rays.

We observed significant variations of the drift times that we related to two kinds of subgrain boundaries typically present in today's CZT detector-grade crystals. The dense networks of low-dislocation-density subgrain boundaries slow down the electrons' drift; high-dislocation-density subgrain boundaries with a few pronounced branches also cause major variations in the drift times.

These variations in drift times, which we have attributed to variations in the electric field, can be explained by the higher conductivity of the subgrain boundaries, in comparison to the bulk, due to their accumulation of impurities and secondary phases that divide the crystal's volume into individual high-resistivity domains. The electric potential along the boundaries set up the boundary conditions that define the electric fields inside individual domains. Consequently, electron clouds move across these regions with different velocities.

Because of the non-uniformity of the electric field, the correction for charge loss due to trapping in thick detectors must rely on measurements of drift time rather than upon the interaction depths.

Acknowledgments

This work was supported by U.S. Department of Energy, Office of Nonproliferation Research and Verification, NA-22 and Defense Threat Reduction Agency. The manuscript has been authored by Brookhaven Science Associates, LLC under Contract No. DE-AC02-98CH1-886 with the U.S. Department of Energy. The United States Government retains, and the publisher, by accepting the article for publication, acknowledges, a world-wide license to publish or reproduce the published form of this manuscript, or allow others to do so, for the United States Government purposes.

References

[1] R. B. James, T. E. Schlesinger, J. C. Lund and M. Schieber, "Cadmium Zinc Telluride Spectrometers for Gamma and X-Ray Applications", in Semiconductors for Room Temperature Nuclear Detector Applications, Vol. 43, edited by R. B. James and T. E. Schlesinger (Academic Press, New York, 1995), p. 334.

[2] G. F. Knoll, *Radiation Detection and Measurement*. 3rd ed. 2000, New York: John Wiley & Sons, Inc.

[3] G. S. Camarda, N. M. Abdul-Jabbar, S. Babalola, A. E. Bolotnikov, Y. Cui, A. Hossain, E. Jackson, H. Jackson, J. R. James, A. L. Luryi, M. Groza, A. Burger, and R. B. James, "Characterization and Measurements of CZT Material: Novel Techniques and Results", in Proceedings of SPIE Hard X-Ray and Gamma-Ray Detector Physics IX, Vol. 6706, edited by R. B. James, A. Burger and L. A. Franks (SPIE, Bellingham, WA, 2007), 670605.

[4] G. S. Camarda, A. E. Bolotnikov, G. A. Carini, and R. B. James, "Effects of Tellurium Inclusions on charge collection in CZT Nuclear Radiation Detectors", in Countering Nuclear and Radiological Terrorism, edited by S. Aprkyan and D. Diamond, Springer, 2006, pp. 199-207.

[5] A. E. Bolotnikov, S. Babalola, G. S. Camarda, Y. Cui, R. Gul, S. U. Egarievwe, P. M. Fochuk, M. Fuerstnau, A. Hossain, F. Jones, K. H. Kim, O. V. Kopach, L. Marchini, B. Raghothamachar, R.Taggart, G. Yang, L. Xu, and R. B. James, "Correlations between crystal defects and performance of CdZnTe detectors", IEEE Trans. Nucl. Sci. 58, pp. 1930-1935, 2011.

[6] P. Rudolph, "Defect formation during crystal growth from the melt", in Springer Handbook of Crystal Growth.

[7] P. Rudolph, "Dislocation cell structures in melt-grown semiconductor compound crystals", Cryst. Res. Technol. 40, pp. 7–20, 2005.

[8] A. E. Bolotnikov, G. S. Camarda, G. A. Carini, M. Fiederle, L. Li, G. W. Wright, and R. B. James, "Performance Studies of CdZnTe Detector by Using a Pulse-Shape Analysis", Proceedings of SPIE Hard X-Ray and Gamma-Ray Detector Physics VII, edited by R. B. James, L. A. Franks, and A. Burger (SPIE, San Diego, CA, 2005), 59200K-1 – 59200K-12.

[9] J. K. Polack, M. Hirt, J. Sturgess, N. D. Sferrazza, A. E. Bolotnikov, S. Babalola, G. S. Camarda, Y. Cui, S. U. Egarievwe, P. M. Fochuck, R. Gul, A. Hossain, K. Kim, O. V. Kopach, L. Marchini, G. Yang, and R. B. James, "Variation of Electric Shielding on Virtual Frisch-grid Detectors," Nuclear Instruments and Methods in Physics Research Section A: Accelerators, Spectrometers, Detectors and Associated Equipment, Volume 621, Issues 1-3, pp. 424-430, 2010.

[10] ?

[11] F. Zhang, C. Herman, Z. He, G. De Geronomo, E. Vernon, and J. Fried, "Characterization of the H3D ASIC readout system and 6.0 cm^3 3-D position sensitive CdZnTe Detectors," IEEE Transactions on Nuclear Science, 2011.

[12] G. S. Camarda, N. M. Abdul-Jabbar, S. Babalola, A. E. Bolotnikov, Y. Cui, A. Hossain, E. Jackson, H. Jackson, J. R. James, A. L. Luryi, M. Groza, A. Burger, and R. B. James, "Characterization and Measurements of CZT Material: Novel Techniques and Results", in Proceedings of SPIE Hard X-Ray and Gamma-Ray Detector Physics IX, Vol. 6706, edited by R. B. James, A. Burger and L. A. Franks (SPIE, Bellingham, WA, 2007), 670605.

[13] A. E. Bolotnikov, S. Babalola, G. S. Camarda, Y. Cui, R. Gul, S. U. Egarievwe, P. M. Fochuk, M. Fuerstnau, A. Hossain, F. Jones, K. H. Kim, O. V. Kopach, L. Marchini, B. Raghothamachar, R.Taggart, G. Yang, L. Xu, and R. B. James, "Correlations between crystal defects and performance of CdZnTe detectors", IEEE Trans. Nucl. Sci. 58, pp. 1930-1935, 2011.

[14] H. F. Matare, "Defects Electronics in Semiconductor", Wiley-Interscience, 1971.

[15] Z. He, W. Li, G. F. Knoll, D. K. Wehe, J. Berry, and C. M. Stahle, "3-D position sensitive CdZnTe gamma-ray spectrometers," Nucl. Instr. and Meth. A 422, pp. 173-178, 1999.

[16] A. E. Bolotnikov, G. S. Camarda, Y. Cui, G. De Geronimo, J. Fried, R. Gul, A. Hossain, K. Kim, G. Yang, E. Vernon, and R. B. James, "Rejecting incomplete charge-collection events in CdZnTe and other semiconductor detectors", Nucl. Instr. and Meth. A 664, pp. 317-323, 2012.